Auxiliary Material

Abrupt change in atmospheric CO_2 during the last ice age

Jinho Ahn[1]*, Edward J. Brook[2], Andreas Schmittner[2] and Karl Kreutz[3]

[1]School of Earth and Environmental Sciences, Seoul National University, Seoul 151742, Korea; [2]College of Earth, Oceanic & Atmospheric Sciences, Oregon State University, Corvallis, Oregon 97331, USA; [3]Climate Change Institute and Department of Earth Sciences, Orono, Maine 04469, USA

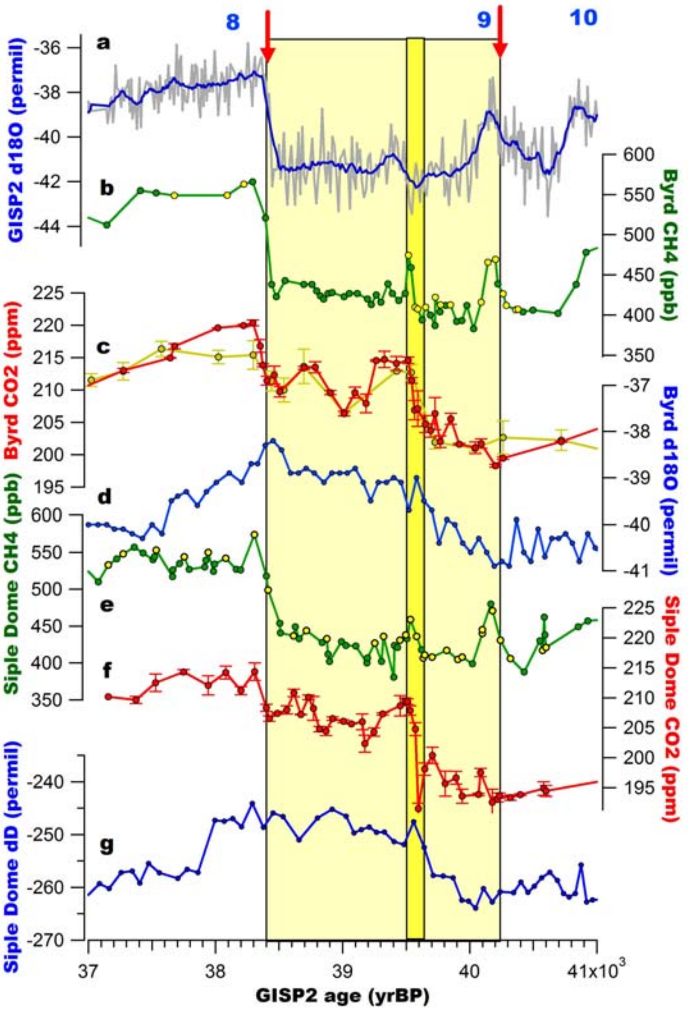

Figure S1. Abrupt atmospheric CO_2 changes. Enlarged plots for records shown in Figure 1. Bright yellow bar points to the timing of abrupt CO_2 changes.

Synchronization of ice core records

We synchronized the Byrd and Siple Dome ice core records to highest the resolution GISP2 $\delta^{18}O_{ice}$ records, which are available at the University of Washington Quarternary Isotope Laboratory website[1] using the official GISP2 time scale at the Greenland Summit Ice Cores CD-ROM[2]. Assuming synchroniety between abrupt warming in Greenland and rapid changes in CH_4, we constructed the Antarctic ice core gas ages by correlating our updated CH_4 records with the GISP2 $\delta^{18}O_{ice}$ record (temperature proxy). The age tie points used are listed in Tables S1. Due to insufficient resolution of the Siple Dome CH_4 records at ~DO12 (Dansgaard-Oeschger event 12), we correlated Siple Dome CO_2 with Byrd CO_2 records, for which gas ages are constructed on the GISP2 time scale via CH_4 correlation. Gas ages between depths of the tie points are linearly interpolated. After determining gas ages, ice ages were determined using published estimates of ice age-gas age difference[3,4].

Table S1. Gas age tie points.

Event	Byrd depth (m)	Siple Dome depth (m)	GISP age[5] (ka)	GICC05[6] (ka)	Gas
DO7 warming	1654.50	810.06	35.32	35.50	CH_4
DO8 warming	1716.46	825.56	38.41	38.22	CH_4
DO9 warming	1759.38	838.28	40.22	40.17	CH_4
DO10 warming	1780.29	846.25	41.18	41.47	CH_4
DO11 warming	1807.95	855.28	42.58	43.42	CH_4
DO12 warming	1863.61		45.39	46.87	CH_4
A2 warming		873.79	45.61	47.11	CO_2
DO14 warming	1960.70		52.22	54.22	CH_4

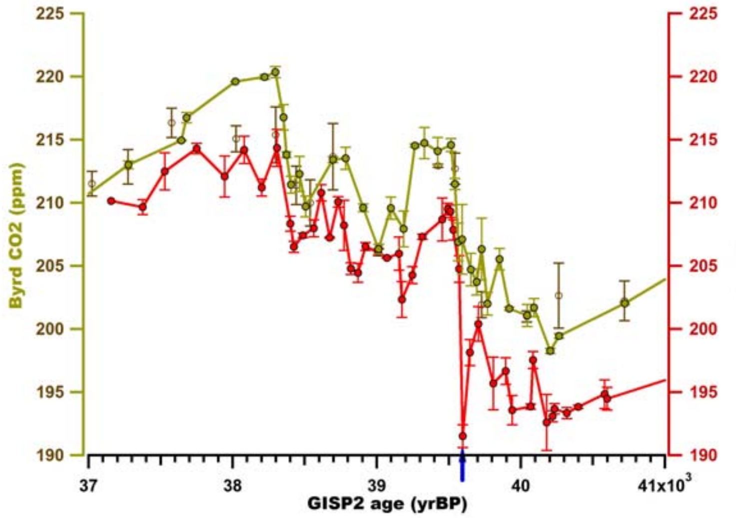

Figure S2. Comparison of Byrd and Siple Dome CO_2 records. CO_2 levels in Byrd are higher than in Siple Dome, but the magnitude and timing of variations and abrupt changes are generally consistent. The Siple Dome record shows the abrupt rise at 39.6 ka was interrupted by a rapid initial drop of ~9 ppm (blue arrow), but this is not confirmed in Byrd ice core. Open circles are previous results for Byrd ice[7].

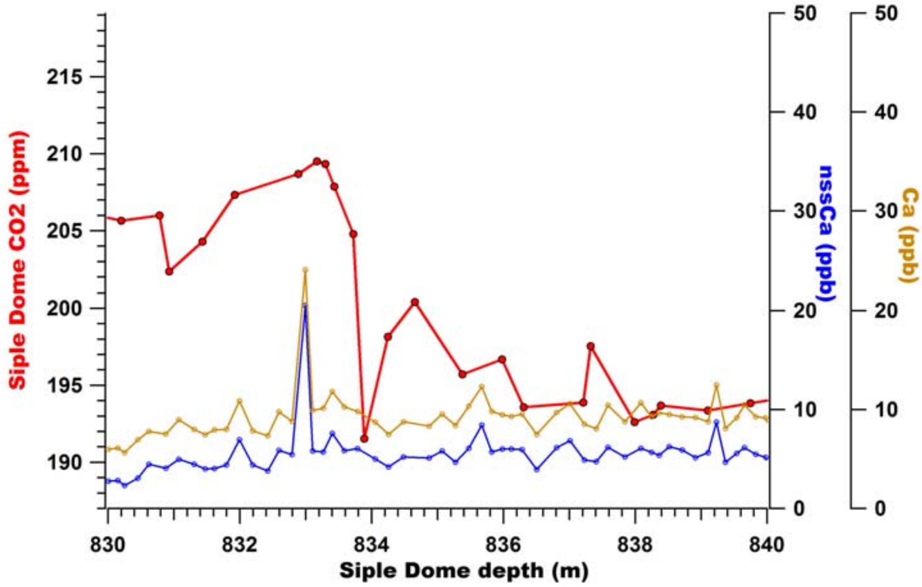

Figure S3. Comparison of atmospheric CO_2, Ca[8] and non-sea-salt (nss) Ca[8] from Siple Dome, Antarctic ice core. There are no significant correlations between abrupt CO_2 change and Ca or nssCa concentration in the ice matrix at ~833.8 m. This indicates that the abrupt CO_2 rise is not likely produced by carbonate-acid reaction in ice.

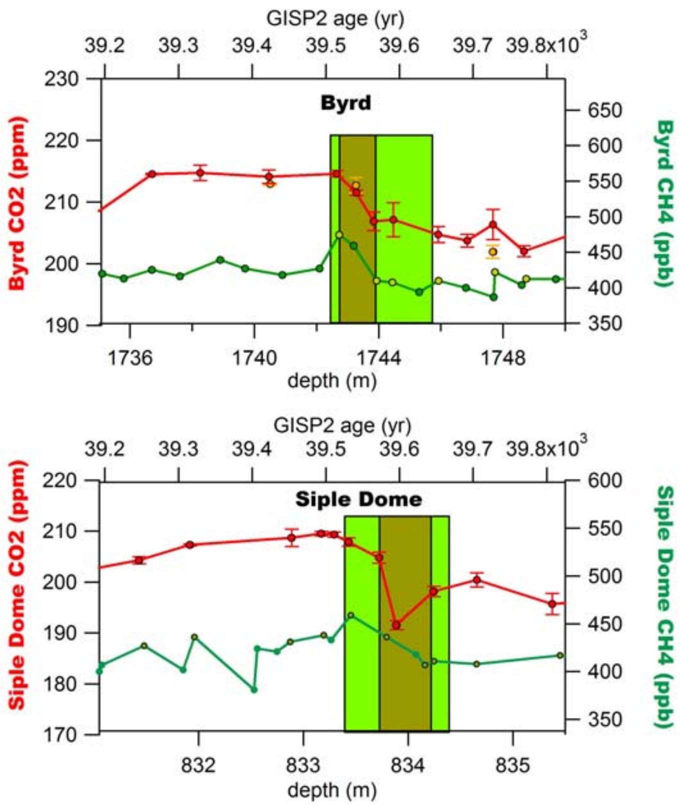

Figure S4. Timing of abrupt CO_2 changes relative to CH_4 plotted on depth and age scales. Green and yellow dots indicate previous and new results respectively. Green and dark yellow boxes specify the time intervals where CO_2 abruptly increased by ~10 ppm and 6~8 ppm, respectively.

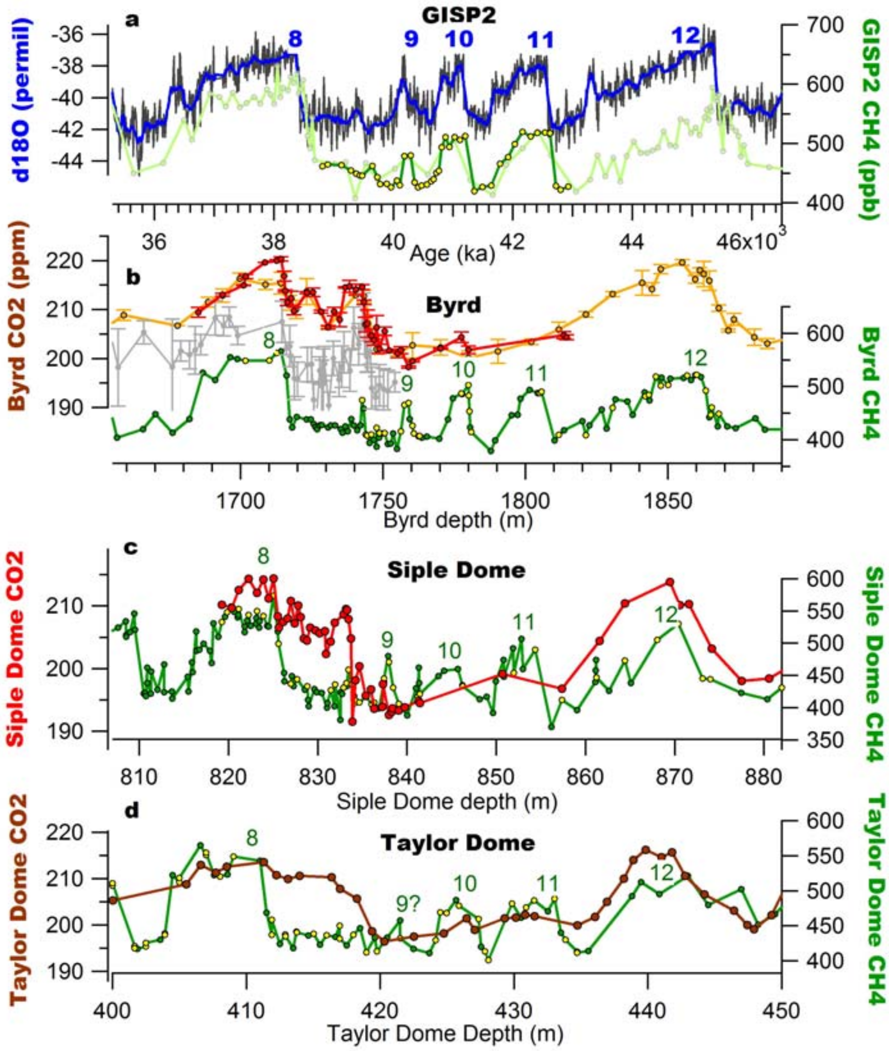

Figure S5. Greenland climate and atmospheric CO_2 and CH_4 records from Antarctic ice cores during Dansgaard-Oeschger events 8~12. a, Greenland isotopic temperature[1,5]. Blue and green numbers indicate the timing of Dansgaar-Oeschger (DO) events. **b~d,** CO_2 (brown or red dots) and CH_4 (green or yellow dots) from Antarctic ice cores. Red CO_2 and yellow CH_4 dots are new data for this study. Orange CO_2 and green CH_4 dots are published data from Byrd[7,4], Siple Dome[3] and Taylor Dome[9,10] ice cores. Gray dots in b indicate previous study results from the University of Bern[11]. Note that Antarctic ice core records are plotted on depth domains.

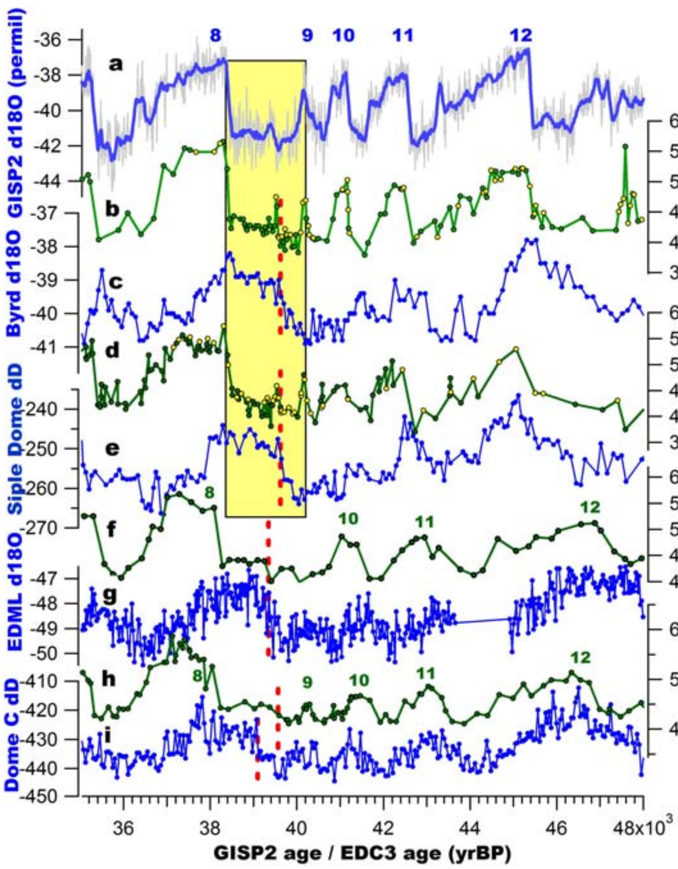

Figure S6. A rapid warming in Antarctica with a synchronous small change in CH_4 between Dansgaard-Oeschger warming events 8 and 9. a, Greenland temperature proxy, $\delta^{18}O_{ice}$[1,5]. **b~i,** CH_4 (green lines) and temperature proxies (blue lines) from Antarctic ice cores. **b&c,** from Byrd ice core[7,4, this study]. **d&e,** from Siple Dome[3, this study]. **f&g,** from EPICA Dronning Maud Land ice core[6]. **h&i,** from EPICA Dome C[12,13] ice core. Yellow dots are new CH_4 records for this study. Red vertical lines present a common time when Antarctica rapidly warmed, CH_4 experienced a step-like rise and CO_2 abruptly changes in between Dansgaard-Oeschger warming events 8 and 9. The Byrd and Siple Dome records are on GISP2 time scale while the EPICA Dronning Maud Land and Dome C records are on GICC05 and EDC3 time scales, respectively. The age offset between the step-like rise of CH_4 and the rapid warming from Dome C records is within the uncertainty in gas age - ice age difference.

Coupled climate-carbon cycle model

We use the UVic Earth System Climate Model[14] version 2.8 in a glacial background climate[15]. The model consists of a simple one-layer, two-dimensional (latitude-longitude) energy-moisture balance atmospheric component with diffusive and advective (using a monthly varying fixed wind climatology) heat and moisture transport, a three-dimensional coarse resolution ocean general circulation model, a dynamic-thermodynamic sea ice model and terrestrial[16] and ocean[17] carbon cycle components. To drive an abrupt change in the system we decreased the global atmospheric albedo over a range of values (Fig. S7). We do not propose albedo change as the ultimate cause of CO_2 variations, we change albedo simply because it is a prescribed parameter in the model that can be can be changed independently. The model uses monthly 2-dimensional (latitude-longitude) maps of atmospheric coalbedo (1-a, where a is the albedo) as input fields in the calculation of the shortwave radiative budget at the top-of-the-atmosphere. These fields were multiplied by constant scaling factors (1.005, 1.006, 1.007, 1.008, and 1.01) corresponding to a 0.5%, 0.6%, 0.7%, 0.8% and a 1% increase. Note that the atmospheric coalbedo is higher (albedo is lower) in areas of sparse cloud cover such as the subtropics and desert regions and lower (albedo is higher) in areas of dense cloud cover such as mid to high latitudes and the tropics. The forcing changes the absorbed shortwave radiation at the top-of-the-atmosphere $F = (1-a)S$, where S is the solar insolation. Since S is higher at low latitudes than at high latitudes the forcing ΔF will also be larger at low latitudes that at high latitudes in contrast to e.g. the radiative forcing from doubling of CO_2, which is globally uniform. Averaged over the Earth's surface area $S = 342$ W/m^2. Hence the globally averaged radiative forcing corresponding to a 1% increase in the coalbedo is $\Delta F = 0.01 \cdot S = 3.4$ W/m^2. Note that this forcing is equivalent to changing the solar insolation S by 1%, a standard forcing used in climate modeling studies, e.g. to evaluate climate sensitivity[18]. This forcing is also equivalent to a globally uniform change in the atmospheric albedo as shown in the upper panel of Fig. S7.

As a response to the increased absorbed solar insolation climate warms in the model, with a global average surface air temperature increase of 0.8°C to 1.6°C (bottom panel in Fig. S7). During the transient phase the warming is not uniform but more pronounced over land than over the ocean with a maximum over Asia and a minimum over the Southern Ocean (Fig. S8). The warming leads to a reduction in sea ice cover in the Southern Ocean and an increase of atmospheric CO_2 (Fig. S9). However, the increase of atmospheric CO_2 is not caused by the reduction in Southern Ocean sea ice cover since the global ocean carbon inventory increases (Fig. S9). Rather warmer land surface temperatures lead to accelerated respiration and carbon loss from soils.

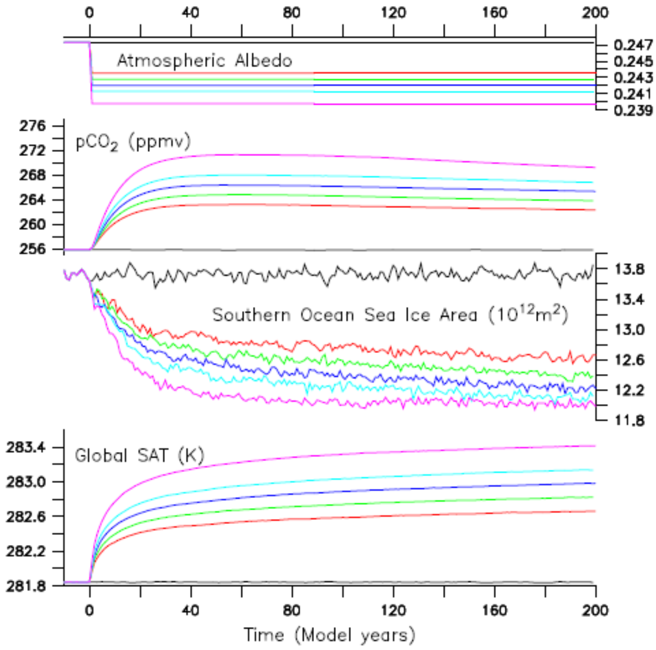

Figure S7. Model results for instantaneous increase of the atmospheric albedo by 0.5% (red), 0.6% (green), 0.7% (blue), 0.8% (lightblue) and 1% (pink) at model year 0. Top panel: resulting change in atmospheric albedo. Second panel from top atmospheric CO_2. Third panel from top: Southern Ocean sea ice area. Bottom panel: Global surface air temperature.

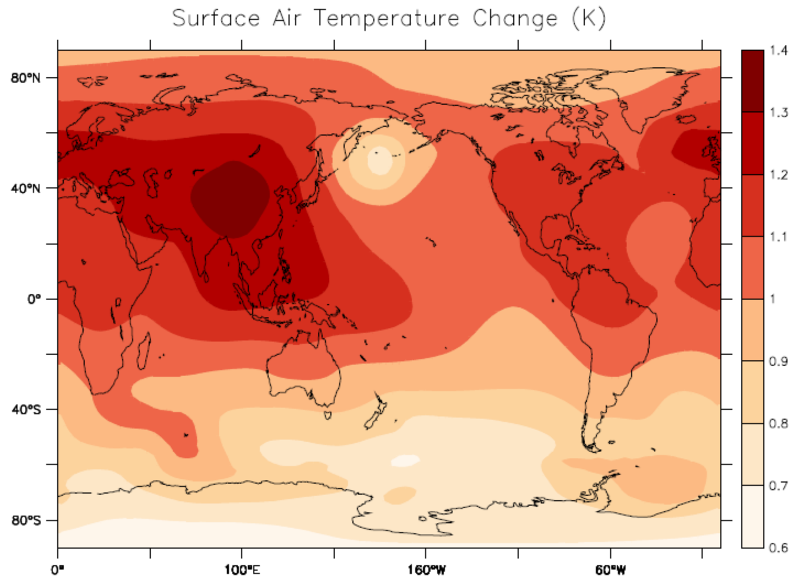

Figure S8. Surface air temperature response 100 years after an instantaneous increase of the atmospheric coalbedo by 0.7% (blue line in Figure S7).

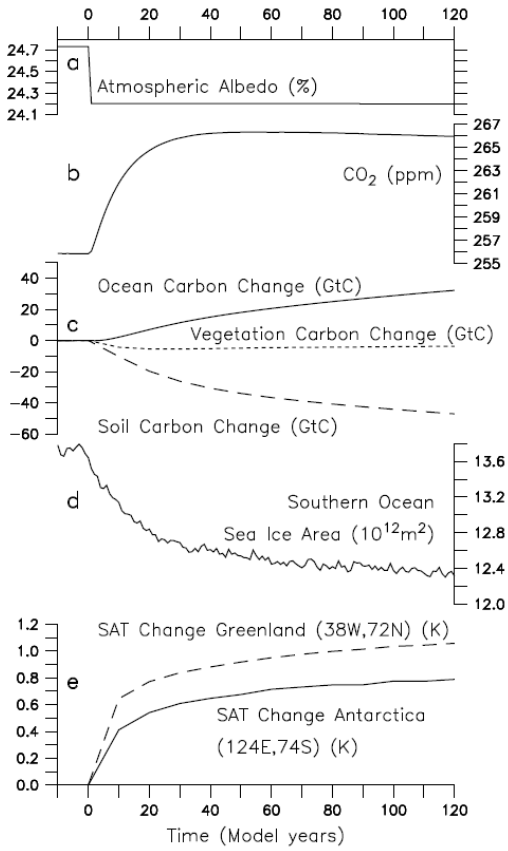

Figure S9. Simulation of abrupt atmospheric CO_2 changed during glacial background climate conditions. Global albedo was decreased by 2% (co-albedo was increased by 0.7%) at model year 0. **a,** atmospheric albedo. **b,** atmospheric CO_2. **c,** Carbon inventories in ocean (black), vegetation (red) and soil (green) in units of Giga tons of carbon (GtC). **d,** Southern Ocean sea ice area. **e,** surface air temperature change in Greenland (red) and Antarctica (black). The model shows that the carbon for the CO_2 rise originates from soil.

Table S2. New CO_2 data for Byrd. Yellow bars indicate reanalyzed ice samples that were previously studied[7] to check reproducibility. Byrd ages are synchronized with GISP2 ice core ages by CH_4 correlation (see "Synchronization of ice core records" section).

depth (m)	GISP2 age (kyrBP)	CO2 (ppm)	# of replicates	uncertainty (ppm)
1685.14	36.848	209.5	2	1.0
1693.71	37.276	213.0	2	0.3
1701.09	37.643	215.0	2	0.1
1701.80	37.679	216.8	2	0.4
1708.62	38.019	219.6	2	0.0
1712.69	38.222	220.0	3	0.2
1714.16	38.295	220.3	4	0.5
1715.30	38.352	216.8	2	1.0
1715.69	38.372	213.8	2	0.2
1716.36	38.404	211.5	2	0.7
1717.70	38.462	212.3	3	1.4
1718.72	38.506	209.7	2	0.8
1723.25	38.696	213.4	2	0.2
1725.33	38.784	213.5	2	0.9
1728.18	38.904	209.6	2	0.3
1730.71	39.011	206.4	3	0.4
1732.76	39.097	209.6	4	0.9
1734.82	39.184	207.9	2	1.4
1736.71	39.264	214.5	2	0.1
1738.26	39.329	214.7	2	1.2
1740.47	39.423	214.1	2	1.1
1742.65	39.515	214.6	4	0.5
1743.28	39.541	211.5	2	0.4
1743.84	39.565	206.9	4	1.5
1744.47	39.591	207.1	5	2.8
1745.91	39.652	204.7	4	1.3
1746.85	39.692	203.7	4	1.0
1747.68	39.726	206.3	3	2.5
1748.67	39.768	202.0	2	0.9
1750.63	39.851	205.5	3	0.9
1752.23	39.918	201.6	2	0.1
1755.18	40.043	201.1	2	0.9
1756.32	40.091	201.7	4	0.7
1758.96	40.202	198.3	2	0.2
1760.32	40.263	199.5	2	0.2

1770.27	40.720	202.0	2	0.1
1777.55	41.054	204.3	2	1.1
1779.96	41.165	201.8	2	0.8
1813.44	42.857	204.8	3	0.7
1814.46	42.909	204.3	3	0.5

Table S3. New CO_2 data for Siple Dome. The ages are synchronized with GISP2 ice core ages by CH_4 correlation (see "Synchronization of ice core records" section).

depth (m)	GISP age (kyrBP)	CO_2 (ppm)	# of replicates	uncertainty (ppm)
819.27	37.156	210.2	1	
820.37	37.374	209.7	3	0.6
821.14	37.529	212.5	2	1.5
822.24	37.749	214.3	3	0.4
823.22	37.943	212.1	5	1.6
823.90	38.080	214.2	2	1.1
824.51	38.201	211.2	2	0.7
825.04	38.307	214.4	2	1.5
825.51	38.400	208.3	2	0.6
825.66	38.424	206.5	2	0.5
826.10	38.487	207.4	2	0.2
826.62	38.561	208.0	2	0.7
827.00	38.615	210.8	2	0.6
827.40	38.672	207.2	2	0.0
827.82	38.732	210.1	3	0.4
828.10	38.771	208.2	2	2.0
828.44	38.819	204.8	2	0.5
828.78	38.868	204.5	4	0.7
829.16	38.922	206.5	3	0.3
829.76	39.008	206.1	3	0.3
830.20	39.070	205.7	2	0.0
830.79	39.154	206.0	3	1.3
830.93	39.174	202.3	2	1.4
831.44	39.246	204.3	2	0.7

831.92	39.315	207.3	2	0.2
832.89	39.453	208.7	2	1.7
833.17	39.493	209.5	2	0.5
833.30	39.511	209.3	2	0.5
833.44	39.531	207.9	2	0.8
833.72	39.572	204.8	5	1.1
833.89	39.595	191.5	2	0.9
834.25	39.646	198.1	4	1.0
834.66	39.705	200.4	2	1.4
835.38	39.807	195.7	3	2.1
835.98	39.893	196.7	2	1.1
836.31	39.940	193.6	2	1.2
837.21	40.068	193.9	3	0.2
837.33	40.084	197.6	3	0.7
837.99	40.178	192.6	3	2.2
838.28	40.219	193.1	2	0.4
838.39	40.233	193.7	2	0.4
839.10	40.319	193.3	2	0.4
839.75	40.397	193.8	2	0.1
841.28	40.581	194.8	2	1.1
841.43	40.599	194.5	2	0.9
850.69	41.868	199.2	3	1.5
857.37	42.922	196.8	2	0.7
861.59	43.613	204.4	2	0.7
864.44	44.079	210.4	2	2.2
869.48	44.904	213.8	2	0.4
870.59	45.086	210.1	2	1.4
871.60	45.252	210.3	3	2.3
874.15	45.799	203.2	3	0.3
877.50	46.521	198.0	2	2.1
880.59	47.186	198.4	2	0.3
903.88	52.191	218.3	2	0.2
905.04	52.441	218.4	2	1.4

Table S4. CH_4 data for Siple Dome. The ages are synchronized with GISP2 ice core ages by CH_4 correlation (see “Synchronization of ice core records” section).

depth (m)	GISP age (kyrBP)	CH_4 (ppb)	Reference
810.890	35.486	462	(3)
810.891	35.486	438	(3)
811.290	35.565	422	(3)
811.330	35.573	456	(3)
812.046	35.716	428	(3)
812.781	35.862	467	(3)
812.801	35.866	424	(3)
813.659	36.038	425	(3)
813.696	36.045	414	(3)
815.435	36.392	448	(3)
815.495	36.404	425	(3)
815.904	36.485	470	(3)
815.994	36.503	455	(3)
816.389	36.582	518	(3)
816.414	36.587	488	(3)
816.730	36.650	490	(3)
817.225	36.748	499	(3)
817.917	36.886	488	(3)
818.126	36.928	469	(3)
818.295	36.962	531	(3)
818.875	37.077	510	(3)
819.270	37.156	533	this study
819.605	37.223	541	(3)
819.865	37.275	548	this study
820.295	37.360	557	(3)
820.640	37.429	549	(3)
821.030	37.507	540	(3)
821.090	37.519	544	(3)
821.160	37.533	553	this study
821.805	37.661	517	(3)
821.825	37.665	526	(3)
822.085	37.717	535	(3)
822.270	37.754	544	this study
822.469	37.794	527	(3)
823.077	37.915	530	(3)
823.117	37.923	539	(3)
823.215	37.943	550	this study
823.427	37.985	524	(3)
823.467	37.993	534	(3)
823.902	38.079	542	this study
824.322	38.163	527	(3)
824.490	38.197	526	(3)

825.043	38.307	574	this study
825.510	38.400	518	(3)
825.593	38.415	499	this study
826.228	38.505	454	(3)
826.268	38.511	441	(3)
827.000	38.615	437	this study
827.083	38.627	449	(3)
827.298	38.657	433	(3)
827.698	38.714	444	this study
828.570	38.838	428	(3)
828.840	38.877	433	this study
828.900	38.885	412	(3)
828.980	38.897	402	(3)
829.635	38.990	429	(3)
829.885	39.025	424	(3)
830.436	39.104	423	(3)
831.052	39.192	400	(3)
831.077	39.195	407	(3)
831.480	39.252	427	this study
831.852	39.305	402	(3)
831.961	39.321	436	this study
832.530	39.402	381	(3)
832.560	39.406	424	(3)
832.750	39.433	421	(3)
832.875	39.451	431	this study
833.195	39.496	438	this study
833.265	39.506	433	(3)
833.455	39.533	459	this study
833.795	39.582	436	this study
834.075	39.622	418	(3)
834.163	39.634	407	this study
834.246	39.646	411	this study
834.655	39.704	408	this study
835.450	39.817	417	this study
836.065	39.905	405	this study
836.310	39.940	408	this study
836.878	40.021	399	(3)
837.423	40.098	440	this study
837.423	40.098	445	this study
837.900	40.166	480	(3)
837.988	40.178	471	this study
838.455	40.241	431	this study
839.100	40.319	406	this study
840.010	40.428	388	(3)
841.030	40.551	430	(3)
841.205	40.572	417	this study
841.315	40.586	462	(3)

841.355	40.590	438	(3)
841.430	40.599	421	this study
843.530	40.852	449	(3)
844.160	40.928	457	(3)
845.706	41.115	460	(3)
846.225	41.177	435	(3)
846.246	41.180	433	this study
848.141	41.473	413	(3)
848.925	41.595	417	(3)
849.651	41.707	392	(3)
849.955	41.754	441	(3)
850.824	41.889	474	(3)
850.865	41.896	448	(3)
851.890	42.054	492	(3)
851.977	42.068	454	this study
852.855	42.204	507	(3)
852.974	42.223	460	(3)
854.353	42.436	490	this study
856.203	42.731	370	(3)
857.370	42.922	412	this study
859.048	43.197	396	(3)
861.095	43.532	440	(3)
861.151	43.541	458	(3)
861.195	43.548	474	(3)
861.213	43.551	447	this study
862.639	43.785	426	(3)
864.435	44.079	473	this study
865.085	44.185	438	(3)
868.055	44.671	505	this study
870.430	45.060	530	this study
873.145	45.504	445	this study
873.995	45.687	444	this study
877.461	46.432	423	(3)
880.371	47.058	413	(3)
881.985	47.403	431	this study
882.830	47.586	375	(3)
886.538	48.384	448	(3)

Table S5. CH_4 data for Byrd Ice core. For ages see "Synchronization of ice core records" section.

depth (m)	**GISP age (kyrBP)**	**CH_4 (ppb)**	**reference**
1656.60	35.425	404	(4)
1665.80	35.884	420	(4)
1670.10	36.098	448	(4)
1676.10	36.397	413	(4)

1682.10	36.696	439	(4)
1686.70	36.926	526	(4)
1691.10	37.145	512	(4)
1696.40	37.410	555	(4)
1698.90	37.534	552	(4)
1701.72	37.675	549	(4)
1710.11	38.093	549	(4)
1712.72	38.223	563	(4)
1714.10	38.292	566	(4)
1716.10	38.392	521	(4)
1717.20	38.441	438	(4)
1718.10	38.479	423	(4)
1719.70	38.547	443	(4)
1723.20	38.694	438	(4)
1724.70	38.758	438	(4)
1725.60	38.795	430	(4)
1726.30	38.825	424	(4)
1726.90	38.850	420	(4)
1727.70	38.884	427	(4)
1728.50	38.918	428	(4)
1730.70	39.011	423	(4)
1731.70	39.053	427	(4)
1733.20	39.116	427	(4)
1735.10	39.196	420	(4)
1735.80	39.226	413	(4)
1736.70	39.264	425	(4)
1737.60	39.302	416	(4)
1738.90	39.356	439	(4)
1739.70	39.390	427	(4)
1740.90	39.441	418	(4)
1742.10	39.491	427	(4)
1742.73	39.518	474	this study
1743.20	39.538	459	(4)
1743.93	39.569	410	this study
1744.44	39.590	408	this study
1745.30	39.626	394	(4)
1745.92	39.652	410	this study
1746.80	39.690	400	(4)
1747.70	39.727	387	(4)
1747.74	39.729	422	this study

1748.60	39.765	404	(4)
1748.74	39.771	413	this study
1749.70	39.812	412	(4)
1750.55	39.848	413	this study
1751.70	39.896	392	(4)
1752.70	39.938	393	(4)
1753.60	39.976	412	(4)
1754.90	40.031	383	(4)
1756.28	40.089	416	this study
1757.55	40.143	466	this study
1758.96	40.202	469	this study
1759.40	40.221	439	(4)
1760.32	40.263	427	this study
1760.83	40.287	412	this study
1762.43	40.360	406	this study
1762.85	40.379	407	this study
1763.70	40.418	404	(4)
1765.40	40.496	406	(4)
1769.70	40.694	402	(4)
1772.80	40.836	438	(4)
1774.50	40.914	478	(4)
1777.52	41.053	487	this study
1777.70	41.061	486	(4)
1779.96	41.165	503	this study
1780.07	41.170	483	this study
1780.40	41.185	454	this study
1780.60	41.196	423	(4)
1781.02	41.217	415	this study
1787.90	41.565	379	(4)
1789.40	41.641	399	(4)
1795.20	41.935	446	(4)
1797.20	42.036	447	(4)
1798.30	42.092	477	(4)
1801.40	42.249	494	(4)
1804.30	42.395	488	(4)
1805.08	42.435	488	this study
1805.70	42.466	490	this study
1810.20	42.694	399	(4)
1811.76	42.772	409	this study
1813.50	42.860	418	(4)

1820.00	43.188	435	(4)
1821.22	43.250	409	this study
1822.50	43.315	427	(4)
1826.80	43.532	457	(4)
1828.50	43.618	421	(4)
1830.66	43.727	460	this study
1831.60	43.774	476	(4)
1835.80	43.986	472	(4)
1837.60	44.077	447	(4)
1841.80	44.289	489	(4)
1842.11	44.305	482	this study
1843.38	44.369	484	this study
1843.60	44.380	474	(4)
1845.76	44.489	519	this study
1847.48	44.576	502	this study
1847.80	44.592	517	(4)
1850.09	44.707	503	this study
1850.80	44.743	515	(4)
1855.60	44.986	516	(4)
1856.83	45.048	521	this study
1858.10	45.112	512	(4)
1859.60	45.188	522	this study
1860.15	45.215	522	this study
1861.60	45.289	518	(4)
1863.33	45.376	492	this study
1864.50	45.453	442	(4)
1865.05	45.491	447	this study
1865.41	45.517	461	this study
1867.50	45.664	425	(4)
1867.95	45.695	449	this study
1870.80	45.896	425	(4)
1873.80	46.107	422	(4)
1880.80	46.599	440	(4)
1884.10	46.831	419	(4)
1891.80	47.373	420	(4)
1892.69	47.436	451	this study
1893.22	47.473	463	this study
1894.21	47.543	472	this study
1894.80	47.584	558	(4)
1895.73	47.650	431	this study

1896.42	47.698	460	this study
1897.15	47.749	480	this study
1897.68	47.787	479	this study
1898.90	47.873	435	(4)
1900.20	47.964	437	this study
1903.70	48.210	442	(4)

Table S6. CH_4 data for Taylor Dome Ice core.

depth (m)	CH_4 (ppb)	Reference
384.50	425	(10)
384.98	400	this study
386.10	398	this study
386.50	375	(10)
387.26	386	this study
387.74	384	(10)
388.50	384	(10)
389.17	411	this study
389.50	397	(10)
389.98	408	this study
390.50	430	(10)
391.03	451	this study
391.50	456	(10)
392.02	440	this study
392.50	397	(10)
392.91	412	this study
393.50	415	(10)
394.83	472	this study
395.50	405	(10)
396.13	424	this study
397.73	438	(10)
397.95	463	this study
399.50	506	(10)
400.00	509	this study
401.66	420	this study
401.86	417	(10)
402.50	423	this study
403.58	430	(10)
403.91	438	this study
404.50	522	(10)

405.00	515	this study
406.56	565	(10)
407.00	553	this study
407.60	522	(10)
408.03	520	this study
408.59	523	(10)
409.05	549	this study
411.04	543	(10)
411.50	469	(10)
411.90	448	this study
412.50	424	(10)
412.93	437	this study
413.50	418	(10)
413.75	441	this study
414.64	436	(10)
415.03	439	this study
415.50	423	(10)
416.00	437	this study
416.66	434	(10)
416.98	441	this study
417.50	422	(10)
418.50	446	(10)
419.60	433	(10)
419.75	414	this study
420.51	433	(10)
421.50	458	(10)
421.50	432	this study
422.50	417	(10)
423.68	411	(10)
424.15	430	this study
425.68	487	(10)
426.43	469	this study
427.54	420	(10)
428.10	401	this study
430.53	462	(10)
431.49	486	this study
432.52	471	(10)
433.03	489	this study

433.50	440	(10)
433.84	430	this study
434.72	412	this study
435.56	414	(10)
438.80	492	(10)
439.50	512	(10)
440.86	495	(10)
442.98	521	(10)
444.52	480	(10)
446.99	502	(10)
448.23	452	(10)
449.50	467	(10)
451.50	507	(10)
448.23	452	(10)
449.50	467	(10)
451.50	507	(10)

Table S7. New CH_4 data for GISP2 Ice core.

Depth (m)	Age[7] (kyrBP)	CH_4 (ppb)
2247.55	38.816	461
2248.55	38.901	464
2251.21	39.131	463
2253.12	39.289	455
2254.25	39.381	449
2254.85	39.435	446
2255.35	39.479	446
2257.05	39.648	462
2257.85	39.732	443
2258.48	39.778	431
2260.05	39.892	432
2261.05	39.964	426
2262.55	40.059	437
2263.55	40.111	430
2264.95	40.184	479
2266.93	40.292	480
2268.05	40.357	435
2269.05	40.415	426
2270.05	40.472	429
2271.55	40.559	431
2273.05	40.630	436

2274.05	40.674	440
2275.05	40.719	450
2276.05	40.763	454
2277.05	40.807	494
2278.55	40.873	510
2280.05	40.938	494
2282.05	41.025	511
2284.05	41.115	506
2286.05	41.205	512
2289.05	41.359	419
2291.20	41.493	426
2293.55	41.639	429
2296.05	41.785	466
2298.60	41.923	477
2301.12	42.035	499
2304.05	42.164	519
2307.05	42.297	512
2309.55	42.408	517
2312.05	42.541	519
2313.55	42.622	517
2315.05	42.720	428
2316.17	42.798	422
2318.05	42.927	427

References

1. http://depts.washington.edu/qil/datasets/gisp2_main.html
2. http://www.ncdc.noaa.gov/paleo/icecore/greenland/summit/document/gispinfo.htm)
3. Brook, E.J. et al. Timing of millennial-scale climate change at Siple Dome, West Antarctica, during the last glacial period. *Quat. Sci. Rev*. **24**, 1333-1343 (2005).
4. Blunier, T. & Brook, E.J. Timing of millennial-scale climate change in Antarctica and Greenland during the last glacial period, *Science* **291**, 109-112, (2001).
5. Grootes, P. M., Stuiver, M., White, J.W.C., Johnsen, S. J. & Jouzel, J. Comparison of the oxygen isotope records from the GISP2 and GRIP Greenland ice cores, *Nature* **366**, 552-554 (1993).
6. EPICA Community members, One-to-one coupling of glacial climate variability in Greenland and Antarctica, *Nature* **444**, 195 (2006).
7. Ahn, J. & Brook, E.J. Atmospheric CO_2 and climate on millennial time scales during the last glacial period, *Science* **322**, 83 (2008).
8. Mayewski, P.A., M. Meredith, C. Summerhayes, J. Turner, S. Aoki, Barrett, P. N.A.N. Bertler et al. State of the Antarctic and Southern Ocean Climate System (SASOCS), Reviews of Geophysics 47, RG1003, doi:10.1029/2007RG000231 (2009).
9. Indermühle, A., Monnin, E., Stauffer, B., Stocker, T.F. & Wahlen, M. Atmospheric CO_2 concentration form 60 to 20 kyr BP from the Taylor Dome ice core, Antarctica, *Geophys. Res. Lett.* **27**, 735 (2000).
10. Brook, E.J., Harder, S., Severinghaus, J., Steig, E.J. & Sucher, C.M. On the origin and timing of rapid climate changes in atmospheric methane during the last glacial period. *Global Biogeochem. Cycles* **14**, 559 (2000).
11. Stauffer, B. et al. Atmospheric CO_2 concentration and millennial-scale climate change during the last glacial period, *Nature* **392**, 59-62 (1998).
12. Jouzel, J. et al. Orbital and millennial Antarctic climate variability over the past 800,000 years, *Science* **317**, 793 (2007).
13. Loulergue, L. et al. Orbital and millennial-scale features of atmospheric CH_4 over the past 800,000 years, *Nature* **453**, 383 (2008).
14. Weaver, A. J., M. Eby, E. C. Wiebe, C. M. Bitz, P. B. Duffy, T. L. Ewen, A. F. Fanning, M. M. Holland, A. MacFadyen, H. D. Matthews, K. J. Meissner, O. Saenko, A. Schmittner, H. X. Wang, and M. Yoshimori (2001), The UVic Earth System Climate Model: Model description, climatology, and applications to past, present and future climates, Atmos Ocean, 39(4), 361-428.
15. Schmittner, A., and E. D. Galbraith (2008), Glacial greenhouse-gas fluctuations controlled by ocean circulation changes, Nature, 456(7220), 373-376.
16. Meissner, K. J., A. J. Weaver, H. D. Matthews, and P. M. Cox (2003), The role of land surface dynamics in glacial inception: a study with the UVic Earth

System Model, Clim Dynam, 21(7-8), 515-537, Doi 10.1007/S00382-003-0352-2.
17. Schmittner, A., A. Oschlies, H. D. Matthews, and E. D. Galbraith (2008), Future changes in climate, ocean circulation, ecosystems, and biogeochemical cycling simulated for a business-as-usual CO_2 emission scenario until year 4000 AD, Global Biogeochem Cy, 22(1), GB1013.
18. Hansen, J., A. Lacis, D. Rind, G. Russell, P. Stone, I. Fung, R. Ruedy, and J. Lerner, Climate sensitivity: Analysis of feedback mechanisms, in *Climate Processes and Climate Sensitivity*, edited by J. E. Hansen and T. Takahashi, pp. 130-163, American Geophysical Union (1984).